Available online at www.sciencedirect.com
SCIENCE DIRECT®
Journal of Organometallic Chemistry 669 (2003) 87–100
Journal of Organometallic Chemistry
www.elsevier.com/locate/jorganchem

The lithiation of arylamines and the preparation of cyclopentadienyltitanium(IV) arylaminate complexes

Anthony G. Avent, Peter B. Hitchcock, G. Jeffery Leigh *, Maria Togrou

School of Chemistry, Physics and Environmental Science, University of Sussex, Brighton BN1 9QJ, UK

Received 15 November 2002; received in revised form 14 December 2002; accepted 14 December 2002

Abstract

The 2-lithio-derivatives of a range of aryl-substituted amines were prepared, generally from the 2-bromo-compounds and butyllithium. These compounds cause dinitrogen uptake when mixed with $[VCl_2(Me_2NCH_2CH_2NMe_2)_2]$ though no dinitrogen complexes were characterised. With $[TiCpCl_3]$ the lithio-derivatives form compounds $[TiCpCl_2(arylaminate)]$ the NMR spectra of which were studied in some detail. The X-ray structures of $[\{LiC_6H_4\text{-}2\text{-}CH_2N(CH_2CH{=}CH_2)_2\}_4]$ and $[TiCp(C_6H_4CH_2R)Cl_2]$ (R = NMe_2, $N(CH_2CH{=}CH_2)_2$ or NC_4H_8O) are described.

Keywords: X-ray structures; Lithiation reaction; Lithio derivatives

1. Introduction

In view of the disappointing experimental results with the ferrocenylaminates and $[VCl_2(tmen)_2]$ in nitrogen-fixation reactions [1], we decided to investigate the ligating properties of the arylaminates $C_6H_4CH_2R^-$ (R = NMe_2, NEt_2, $N(CH_2CH{=}CH_2)_2$, NC_4H_8O or $NMeCH_2Ph$) in the hope that these would yield cleaner and more reactive systems than the ferrocene compounds. The lithiation of $C_6H_5CH_2NMe_2$ is considerably slower than that of $[Fe(C_5H_5)(C_5H_4CH_2NMe_2)]$ under the same conditions. Therefore, the 2-bromo-derivatives of a range of arylamines were lithiated. The 2-lithio-salts precipitated out cleanly from hexane solutions in high yield.

The lithiation of *N*,*N*-dimethylbenzylamine with $LiBu^n$ in anhydrous diethyl ether [2] yields a product, $[(LiC_6H_4\text{-}2\text{-}CH_2NMe_2)_4]$, with a solid state structure containing a tetranuclear aryllithium cluster [3]. The four lithium atoms form an approximately regular tetrahedron. Each of the $C_6H_4CH_2NMe_2$ moieties is bonded to the Li_4 tetramer through a carbon atom that interacts with a face defined by three Li atoms. It also bonds to the cluster via the lone pair of the amine nitrogen, but only to one of these three Li atoms. In strongly coordinating thf, the intra-aggregate solvation in $[(LiC_6H_4\text{-}2\text{-}CH_2NMe_2)_4]$ is replaced by external solvent coordination, affording a dinuclear species, $[\{(LiC_6H_4\text{-}2\text{-}CH_2NMe_2)(thf)_2\}_2]$ [3–5].

There is considerable literature on $1,2\text{-}C_6H_4CH_2NMe_2^-$ as a ligand, first exploited by Manzer et al. [6], and derivatives with many transition metals have been reported (for example, Cr [7], Mo [8], W [9], Mn [10], Ir [11], Pd [12], Pt [13], Cu [14], Au [15], though this is not a comprehensive list). $1,2\text{-}C_6H_4CH_2NMe_2^-$ generally acts as a bidentate ligand, with an *ortho*-carbon atom and the amine nitrogen acting as donors to a transition metal ion, though monodentate coordination is sometimes observed [16].

Our particular interest has been vanadium and titanium chemistry. $[VCl_2(tmen)_2]$ and $LiC_6H_4\text{-}2\text{-}CH_2NMe_2$ yield $[\{V(C_6H_4CH_2NMe_2)_2(py)\}_2(\mu\text{-}N_2)]$, shown to contain bidentate $C_6H_4CH_2NMe_2^-$ [17], and which reacts with CuCl to form the vanadium(III) complex $[VCl(C_6H_4CH_2NMe_2)_2(py)]$ [18]. The dinitrogen complex has an octahedral geometry around the vanadium atom. In addition, the structures of the complexes $[V(C_6H_4CH_2NMe_2)_2(py)_2]$ [19] and $[V(C_6H_4CH_2NMe_2)\{N(SiMe_3)_2\}_2]$ [20] have been reported. A number of titanium complexes containing $C_6H_4CH_2NMe_2^-$ have

* Corresponding author.
E-mail address: g.j.leigh@sussex.ac.uk (G.J. Leigh).

0022-328X/03/$ - see front matter © 2003 Elsevier Science B.V. All rights reserved.
doi:10.1016/S0022-328X(02)02222-2

been synthesised, including the green paramagnetic [TiCp($C_6H_4CH_2NMe_2$)$_2$] [6], bearing two bidentate arylaminate moieties, and the purple complex [TiCp$_2$($C_6H_4CH_2NMe_2$)] [21–23], containing one bidentate arylaminate moiety. The titanium(IV) complex [Ti($C_5Me_4SiMe_2NCH_2Ph$)($C_6H_4CH_2NMe_2$)Cl] has [24] a Ti–NMe_2 interaction with a square-pyramidal coordination around the metal atom.

This paper focuses on an investigation of the ligating properties of the arylaminates $C_6H_4CH_2R^-$ (R = NMe_2, NEt_2, $N(CH_2CH{=}CH_2)_2$, NC_4H_8O or $NMeCH_2Ph$) with titanium(IV). The dinitrogen uptake from the reaction of [VCl_2(tmen)$_2$] with two equivalents of LiC_6H_4-2-CH_2R in thf is also reported.

2. Results and discussion

The lithium compounds LiC_6H_4-2-CH_2NMe_2 (**I**), LiC_6H_4-2-CH_2NEt_2 (**II**), LiC_6H_4-2-$CH_2N(CH_2CH{=}CH_2)_2$ (**III**), LiC_6H_4-2-$CH_2NC_4H_8O$ (**IV**) and LiC_6H_4-2-CH_2NMeCH_2Ph (**V**) were synthesised by reported methods [25,26]. Addition of exactly one equivalent of *n*-butyllithium to the bromoarylamines BrC_6H_4-2-CH_2R (R = NEt_2, $N(CH_2CH{=}CH_2)_2$, NC_4H_8O or $NMeCH_2Ph$) afforded high yields of the corresponding lithium complexes LiC_6H_4-2-CH_2R. LiC_6H_4-2-CH_2NEt_2 (**II**) may also be obtained by a direct *ortho*-lithiation reaction of the corresponding arylamine with one equivalent of tertiary butyllithium [26], but this procedure, due to its much longer reaction time (3–7 days instead of 12–24 h) and lower yields, is less suitable. An attempt was made to prepare LiC_6H_4-2-$CH_2NC_4H_8O$ (**IV**) from $C_6H_5CH_2NC_4H_8O$ and *n*-butyllithium in Et_2O. The product was isolated in a much lower yield and was not as pure as the salt obtained from the reaction with the corresponding brominated arylamine. The halide–lithium exchange reaction rather than lithiation was employed for the preparation of the Li-salts.

The aryllithium complexes LiC_6H_4-2-CH_2R are air- and moisture-sensitive white solids. Complex **II** is readily soluble in Et_2O and only slightly soluble in benzene. Complex **III** is very soluble in Et_2O, hexane or benzene. Complexes **IV** and **V** are insoluble in Et_2O, hexane or benzene, whereas they are readily soluble in thf.

Compound **III** crystallises from a concentrated hexane solution at −20 °C as colourless plates suitable for X-ray structural determination (see Fig. 1). The structure of this complex is analogous to that reported for [($LiC_6H_4CH_2NMe_2$)$_4$] [3]. Selected bond lengths and angles are listed in Table 1. The four Li atoms in **III** form an approximately regular tetrahedron, similar to that found in [(LiMe)$_4$]·2tmen [27], [{LiPh(OEt_2)}$_4$] [28], [(LiC ≡ CPh)$_4$]·2tmen [29] and [($LiC_6H_4CH_2NMe_2$)$_4$] [3]. There are two independent Li–Li distances of 2.453(10) and 2.642(10) Å, while in [($LiC_6H_4CH_2NMe_2$)$_4$] the Li–Li bond lengths are 2.489 and 2.557 Å. Each of the $C_6H_4CH_2N(CH_2CH{=}CH_2)_2$ moieties is bonded to a face of the Li_4 tetramer via a C(aryl) and also via the lone pair of the $N(CH_2CH{=}CH_2)_2$ nitrogen atom to one of these three Li atoms (Fig. 1). There are two independent Li–C distances of 2.276(6) and 2.363(7) Å, compared to three in [($LiC_6H_4CH_2NMe_2$)$_4$] (2.254, 2.290 and 2.305 Å). The Li–Li and Li–C distances reported in other organolithium compounds [28,30], and [($LiCH_2CH_2CH_2NMe_2$)$_4$] (Li–Li 2.492 Å, Li–C 2.266 Å) [31] are not very different from those found in **III**. The Li–N distance in **III** is 2.065 Å, which is slightly longer than the Li–N distance reported for [($LiC_6H_4CH_2NMe_2$)$_4$] (2.011 Å), and the same as that reported for [($LiCH_2CH_2CH_2NMe_2$)$_4$] [31]. The internal phenyl ring angle centred at the ligating carbon atom, C(1)–C(2)–C(3), is remarkably small (111.4(3)°), but similar values have been found in [($LiC_6H_4CH_2NMe_2$)$_4$] (111.7°) [3], [(LiPh)$_2$]·2tmen (111.8°) [32] and [$Li_2Mg_2Ph_6$]·2tmen (111.6°) [33]. Neither the introduction of the heteroatom (N or O) nor the change from an aryl to an alkyl substituent has any significant influence on the structure.

^{1}H- and ^{13}C{^{1}H}-NMR data for [{$LiC_6H_4CH_2N(CH_2CH{=}CH_2)_2$}$_4$] (**III**) recorded in C_6D_6 at 25 °C are listed in Table 2. The dissymmetry of the Li_4 aggregate renders the ArCH_2N protons prochiral and the $N(CH_2CH{=}CH_2)_2$ groupings diastereotopic. Similar NMR data were obtained for the analogous complex [(LiC_6H_3–2-CH_2NMe_2-5-Me)$_4$] dissolved in toluene-d_8.[3,34]. The ^{1}H-NMR spectrum of **III** shows a characteristic low-field chemical shift (δ = 8.41–8.43 ppm) for the aromatic proton (H6). The chemical shifts of the $NCH_2CH{=}CH_2$ and $NCH_2CH{=}CH_2$ protons of one of the allyl groups are close together, generating a rather complex pattern, but the resonances can all be assigned. The simulated spectrum of the allyl group using appropriate chemical shifts and coupling constants compares very well with the experimental spectrum.

The ^{1}H-NMR signals of **III** exhibit dynamic behaviour. At 50 °C the signals due to the protons of the allyl groups show considerable line broadening, while the signals due to the ArCH_2N protons are very sharp. At 30 °C there is evidence from saturation transfer that the two allyl groups inter-exchange. A plausible mechanism of exchange for the allyl groups is shown in Scheme 1. This assumes that the tetramer breaks up in solution, as shown in the case of [(LiC_6H_4-2-CH_2NMe_2)$_4$] [3–5]. We suggest reversible dissociation of the Li–N bond, followed by inversion at the nitrogen atom (and then rotation about an N–C bond) and then reformation of the Li–N bond. Similar dissociative processes have been observed by NMR spectroscopy for several arylaminate M–N chelate complexes [35].

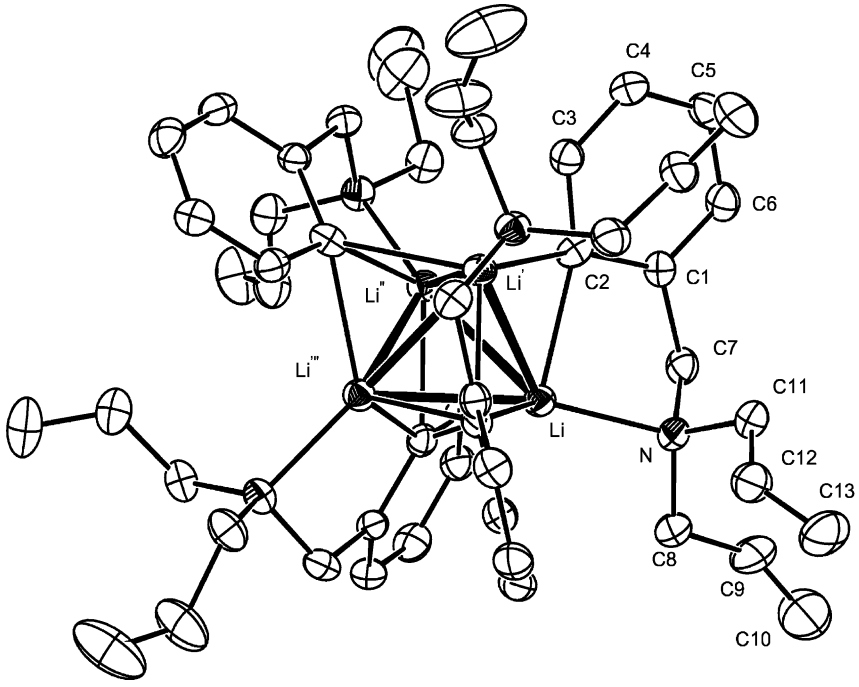

Fig. 1. The molecular structure of $[\{LiC_6H_4CH_2N(CH_2CH{=}CH_2)_2\}_4]$ (**III**), showing the atom labelling scheme.

Table 1
Selected bond lengths (Å) and bond angles (°) for $[\{LiC_6H_4CH_2N(CH_2CH{=}CH_2)_2\}_4]$ (**III**) (e.s.d.s are in parentheses)

Bond lengths			
Li–N	2.065(6)	N–C(11)	1.478(5)
Li–C(2)	2.276(6)	C(2)–Li′	2.276(6)
Li–C(2)′	2.276(6)	C(2)–Li″	2.363(7)
Li–C(2)‴	2.363(7)	C(1)–C(7)	1.519(5)
Li···Li′	2.453(10)	C(8)–C(9)	1.506(7)
Li···Li″	2.642(9)	C(9)–C(10)	1.155(9)
Li···Li‴	2.642(10)	C(11)–C(12)	1.477(6)
N–C(7)	1.481(4)	C(12)–C(13)	1.311(6)
N–C(8)	1.499(5)		
Bond angles			
N–Li–C(2)	87.9(2)	C(1)–C(2)–Li	96.9(2)
N–Li–C(2)′	124.1(3)	C(3)–C(2)–Li′	82.7(2)
N–Li–C(2)‴	118.1(3)	C(1)–C(2)–Li′	150.3(3)
C(2)–Li–C(2)′	113.0(2)	Li–C(2)–Li′	65.2(2)
C(2)–Li–C(2)‴	105.6(2)	C(3)–C(2)–Li″	101.8(3)
C(2)′–Li–C(2)‴	105.6(2)	C(1)–C(2)–Li″	128.6(3)
C(7)–N–C(8)	110.4(3)	Li–C(2)–Li″	69.4(2)
C(7)–N–C(11)	107.9(3)	Li′–C(2)–Li″	69.4(2)
C(8)–N–C(11)	111.7(3)	N–C(7)–C(1)	112.3(3)
Li–N–C(7)	96.4(2)	N–C(8)–C(9)	116.4(4)
Li–N–C(8)	108.0(3)	N–C(11)–C(12)	114.3(3)
Li–N–C(11)	121.1(3)	C(8)–C(9)–C(10)	131.4(7)
C(2)–C(1)–C(7)	119.6(3)	C(11)–C(12)–C(13)	123.4(5)
C(6)–C(1)–C(7)	117.2(3)	Li–Li′–Li″	55.3
C(3)–C(2)–C(1)	111.4(3)	Li–Li′–Li‴	62.3
C(3)–C(2)–Li	147.9(3)		

The ^{1}H-NMR spectrum of $[(LiC_6H_4\text{-}2\text{-}CH_2NEt_2)_4]$ (**II**) in C_6D_6 at 25 °C shows a similar exchange of the ArCH_2N and NCH_2CH_3 groups.

Table 2
^{1}H- and ^{13}C{^{1}H}-NMR data for $[\{LiC_6H_4CH_2N(CH_2CH{=}CH_2)_2\}_4]$ (**III**) in C_6D_6 (in ppm, δ-scale, 25 °C); for the atom labelling scheme used see Scheme 4.1

Proton or carbon	Chemical shifts	
	^{1}H-NMR	^{13}C{^{1}H}-NMR
NCH_2CH=CH_2	2.38–2.42 (m, 1H)	54.8
	2.56–2.59 (m, 1H)	57.9
	2.71–2.75 (dd, 1H)	
	2.95–2.99 (m, 1H)	
ArCH_2N	3.20 (d, 1H, $^2J = 13.2$ Hz)	63.79
	4.61 (d, 1H, $^2J = 13.2$ Hz)	
NCH$_2$CH=CH_2	4.66–4.78 (m) [a]	119.0
	4.87–4.93 (m, 2H)	
NCH$_2$$CH$=CH$_2$	– [a,b]	133.0
	5.31–5.40 (m, 1H)	133.8
Position 3, 4, 5	7.13–7.16 (m, 2H)	125.9
	7.20–7.23 (m, 1H)	126.5
		128.3
Position 6	8.41–8.43 (m, 1H)	140.1
Position 2	–	152.2
Position 1	–	174.47 (br)

[a] Block of 3H.
[b] Signal is hidden beneath the multiplet in the region $\delta = 4.66$–4.78 ppm.

All the lithiated materials were allowed to react with *trans*-$[VCl_2(tmen)_2]$ under dinitrogen and the gas uptake was determined. The method used was that described in Ref. [1]. Although most of the systems can potentiate dinitrogen uptake, it was always less than the one molecule of N_2 per two vanadium atoms consistent with the formation of a bridging dinitrogen complex. The systems seem to undergo side reactions, consistent

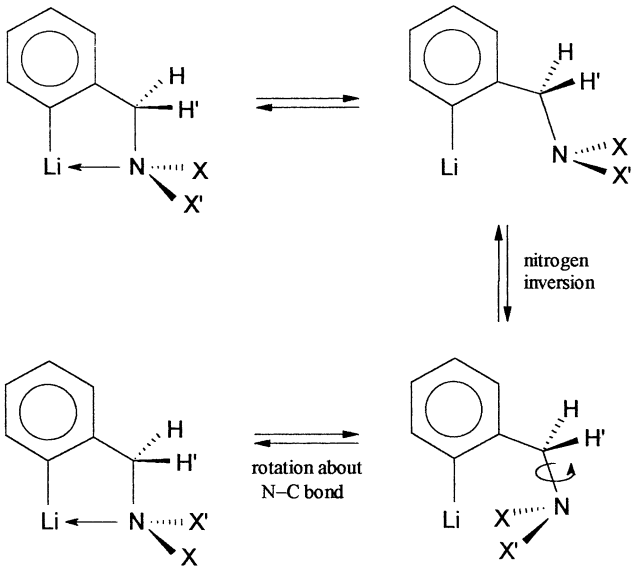

$X = X' = CH_2CHCH_2$

Scheme 1.

with previous reports [36]. The highest N_2 uptake was observed for the system containing vanadium(II) and LiC_6H_4-2-CH_2NMe_2 (up to one molecule of N_2 per four vanadium atoms). In contrast, when $[VCl_2(tmen)_2]$ was mixed with LiC_6H_4-2-$CH_2N(CH_2CH{=}CH_2)_2$ no N_2 uptake was observed. The data are summarised as dinitrogen actually taken up as a percentage of that required to form a V–N_2–V system: LiC_6H_4-2-CH_2R; $R = NMe_2$ (45%), $R = NEt_2$ (15%), $R = N(CH_2CH{=}CH_2)_2$ (0%), $R = NC_4H_8O$ (20%), $R = NMeCH_2Ph$ (35%). No dinitrogen complexes were isolated. This is very similar to our observations with the analogous ferrocenylaminato-complexes [1].

The reaction of $[TiCpCl_3]$ with one molar equivalent of LiC_6H_4-2-CH_2R in diethyl ether proceeds easily at room temperature to give the orange-red Ti^{IV} complexes $[TiCp(C_6H_4CH_2R)Cl_2]$ ($R = NMe_2$ (**VI**), NEt_2 (**VII**), $N(CH_2CH{=}CH_2)_2$ (**VIII**), NC_4H_8O (**IX**) or $NMeCH_2Ph$ (**X**)), which were isolated in good yield. EIMS and IR data are consistent with the proposed formulations Complexes **VI-X** are moderately air- and moisture-sensitive materials, which have good solubility in thf and low solubility in pentane and hexane.

A by-product of the reaction of $[TiCpCl_3]$ with LiC_6H_4-2-$CH_2N(CH_2CH{=}CH_2)_2$ is the purple complex $[TiCpCl_2]$ [37], which was isolated in approximately 20% yield. The organolithium compound clearly causes reduction $Ti^{IV} \rightarrow Ti^{III}$. None of the compounds **VII**–**X** is particularly stable in solution and the ^{1}H-NMR spectra of **VII**–**X** recorded a few days after the preparation of the samples showed signals assigned to $C_6H_5CH_2R$. Compound **VIII** gradually decomposes in the solid state at ambient temperature over 2–3 weeks, while the other complexes of the series are more stable in the solid state, though sometimes not stable long enough to obtain good CHN analyses at a commercial analytical laboratory. They are even less stable in solution. Perhaps the basicity of the arylaminate fragment favours decomposition of the products through abstraction of a proton (from the solvent or from another arylaminate ligand), with regeneration of neutral $C_6H_5CH_2R$. This kind of decomposition is not unprecedented [38].

The X-ray structures of **VI**, **VIII** and **IX** are illustrated in Figs. 2–4. Selected bond lengths and angles are summarised in Tables 3–5. In all of these complexes the arylaminate ligand is *C,N*-bidentate. Variation of the substituents on the nitrogen atom affects the Ti–N bond lengths only slightly.

The coordination geometry around the titanium atom in **VI**, **VIII** and **IX** is best described as square-pyramidal, with the cyclopentadienyl ring in the apical position. Distortions at the base of the pyramid are due to the steric demands of the chelate ring and the repulsion between the two chloride ions. This arrangement was also found in the related compound $[TiCp(Fc'CH_2$-NMe_2-*C,N*$)Cl_2]$ [37].

The chelate ring is non-planar, having an envelope conformation with the amine nitrogen atom displaced 0.65 Å (**VI** and **VIII**) or 0.69 Å (**IX**) out of the mean plane of the other four atoms, which is itself an extension of the plane of the C_6H_4 ring. The five-membered metallocycle in **VI** is characterised by a 39° fold between the Ti, C(1), C(2), C(7) plane and the Ti, N, C(7) plane, while the corresponding dihedral angles in **VIII** and **IX** are 39° and 41°, respectively.

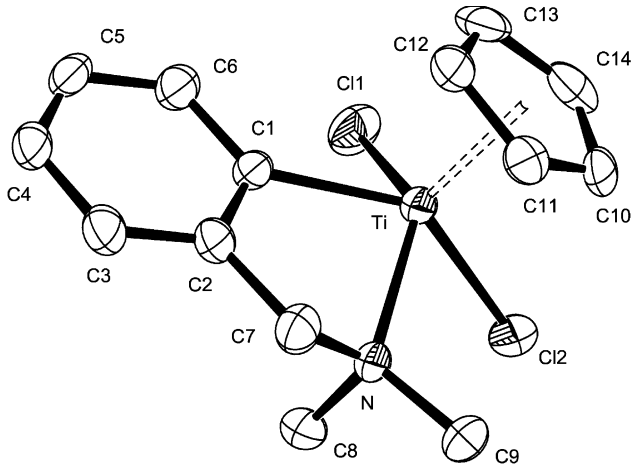

Fig. 2. Plot of the molecular structure of [TiCp($C_6H_4CH_2NMe_2$)Cl_2] (**VI**), showing the atom labelling scheme.

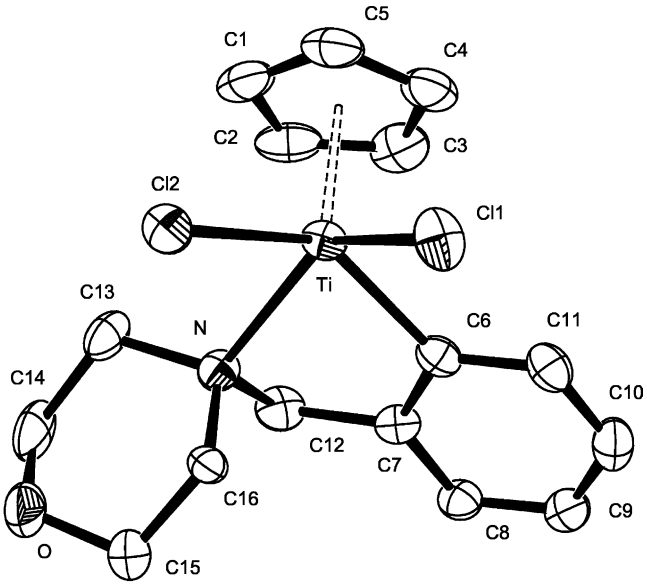

Fig. 4. Plot of the molecular structure of [TiCp($C_6H_4CH_2NC_4H_8$-O)Cl_2] (**IX**), showing the atom labelling scheme.

The Ti–C(1) distances in **VI** is 2.175(6) Å, while the corresponding bond lengths in **VIII** and **IX** are 2.171(4) and 2.175(6) Å, respectively. These distances are longer than those found in [Ti(tbmp)($C_6H_4CH_2NMe_2$-*C,N*)Cl] (2.143 Å) [39] and [Ti(mbp)($C_6H_4CH_2NMe_2$-*C,N*)(O-SO_2CF_3)] (2.116 Å) [40], and slightly shorter than those reported for [Ti($C_5Me_4SiMe_2NCH_2Ph$)($C_6H_4CH_2$-NMe_2-C,N)Cl] (2.195 Å) [24], [TiCp($C_6H_4CH_2NMe_2$-C,N)$_2$] (2.197 Å) [6] and [TiCp$_2$($C_6H_4CH_2NMe_2$-*C,N*)] (2.22 Å) [22].

The Ti–M(1) distances are in the range expected for a Ti^{IV}Cp complex [41]. The average Ti–Cl distance does not change significantly in the range of complexes. The values compare reasonably well with the corresponding dimensions in [TiCp(Fc′CH_2NMe_2-*C,N*)Cl_2}] (2.320 Å) [36] and [Ti($C_5Me_4SiMe_2NCH_2Ph$)($C_6H_4CH_2NMe_2$-*C,N*)Cl] (2.299 Å). The Ti–Cl bond length in [TiCpCl_3] (starting material) is 2.223 Å [42], and the lengthening observed in **VI**, **VIII** and **IX** is probably due to the bulky bidentate arylaminate.

Structures analogous to **VI**, **VIII** and **IX** are proposed for **VII** and **X**, giving an overall electron-count of 14. Monodentate coordination would imply electron-deficient 12e$^-$ species, though this is not uncommon among early transition metals. Coordination of the amino

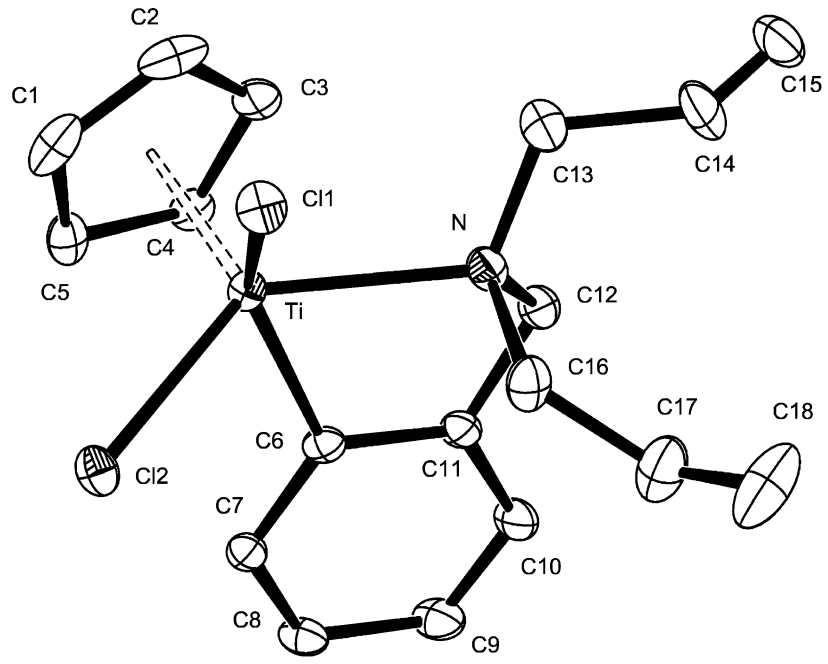

Fig. 3. Plot of the molecular structure of [TiCp{$C_6H_4CH_2N(CH_2CH{=}CH_2)_2$}$Cl_2$] (**VIII**), showing the atom labelling scheme.

Table 3
Selected bond lengths (Å) and bond angles (°) for [TiCp($C_6H_4CH_2NMe_2$)Cl_2] (**VI**) (e.s.d.s are in parentheses)

Bond lengths			
Ti–Cl(1)	2.299(2)	Ti–C(12)	2.372(6)
Ti–Cl(2)	2.372(2)	Ti–C(13)	2.343(6)
Ti–C(1)	2.175(6)	Ti–C(14)	2.323(6)
Ti–N	2.269(5)	N–C(7)	1.483(8)
Ti–M(1)[a]	2.030(6)	N–C(8)	1.497(7)
Ti–C(10)	2.357(6)	N–C(9)	1.496(7)
Ti–C(11)	2.377(6)	C(2)–C(7)	1.490(8)
Bond angles			
M(1)–Ti–C(1) [a]	105.6(2)	C(7)–N–C(8)	108.1(4)
M(1)–Ti–N [a]	112.4(2)	C(7)–N–C(9)	108.4(5)
M(1)–Ti–Cl(1) [a]	112.9(2)	C(8)–N–C(9)	107.3(4)
M(1)–Ti–Cl(2) [a]	111.7(2)	C(7)–N–Ti	108.7(3)
C(1)–Ti–N	74.7(2)	C(8)–N–Ti	104.3(4)
C(1)–Ti–Cl(1)	86.4(2)	C(9)–N–Ti	119.5(4)
C(1)–Ti–Cl(2)	141.5(2)	C(2)–C(1)–Ti	116.3(4)
N–Ti–Cl(1)	134.1(1)	C(6)–C(1)–Ti	127.3(5)
N–Ti–Cl(2)	82.5(13)	C(1)–C(2)–C(7)	116.1(5)
Cl(1)–Ti–Cl(2)	87.7(7)	N–C(7)–C(2)	109.7(5)

[a] M(1) is the centroid of the C(10)-to-C(14) ring.

Table 4
Selected bond lengths (Å) and bond angles (°) for [TiCp{$C_6H_4CH_2N(CH_2CH{=}CH_2)_2$}$Cl_2$] (**VIII**) (e.s.d.s are in parentheses)

Bond lengths			
Ti–Cl(1)	2.365(13)	Ti–C(5)	2.343(4)
Ti–Cl(2)	2.325(13)	N–C(12)	1.495(6)
Ti–C(6)	2.171(4)	N–C(13)	1.503(7)
Ti–N	2.280(3)	N–C(16)	1.525(6)
Ti–M(1) [a]	2.045(4)	C(11)–C(12)	1.489(6)
Ti–C(1)	2.330(5)	C(13)–C(14)	1.503(8)
Ti–C(2)	2.373(5)	C(14)–C(15)	0.998(10)
Ti–C(3)	2.394(4)	C(16)–C(17)	1.512(8)
Ti–C(4)	2.377(4)	C(17)–C(18)	1.212(9)
Bond angles			
M(1)–Ti–C(6) [a]	102.9(2)	C(12)–N–C(16)	110.3(4)
M(1)–Ti–N [a]	114.1(2)	C(13)–N–C(16)	111.7(4)
M(1)–Ti–Cl(1) [a]	112.0(2)	C(12)–N–Ti	108.5(3)
M(1)–Ti–Cl(2) [a]	113.4(2)	C(13)–N–Ti	115.5(3)
C(6)–Ti–N	74.5(16)	C(16)–N–Ti	100.6(2)
C(6)–Ti–Cl(1)	144.3(12)	C(6)–C(11)–C(12)	116.4(4)
C(6)–Ti–Cl(2)	85.4(12)	C(10)–C(11)–C(12)	122.5(4)
N–Ti–Cl(1)	84.2(10)	C(11)–C(12)–N	109.3(3)
N–Ti–Cl(2)	131.3(10)	C(14)–C(13)–N	116.6(5)
Cl(1)–Ti–Cl(2)	87.7(5)	C(15)–C(14)–C(13)	141.0(9)
Cl(1)–Ti–C(4)	140.4(12)	C(17)–C(16)–N	117.3(4)
C(12)–N–C(13)	109.8(3)	C(18)–C(17)–C(16)	127.0(7)

[a] M(1) is the centroid of the C(1)-to-C(5) ring.

group to the metal atom may be essential for complex stabilisation.

The solution behaviour of compounds **VI**–**X** was studied by NMR spectroscopy. They exhibit fluxional behaviour (temperature-dependent broadening of resonances). At high temperatures the ^{1}H-NMR spectra of

Table 5
Selected bond lengths (Å) and bond angles (°) for [TiCp($C_6H_4CH_2NC_4H_8O$)Cl_2] (**IX**) (e.s.d.s are in parentheses)

Bond lengths			
Ti–Cl(1)	2.308(2)	Ti–C(5)	2.336(6)
Ti–Cl(2)	2.388(2)	N–C(12)	1.499(9)
Ti–C(6)	2.175(6)	N–C(13)	1.503(7)
Ti–N	2.303(5)	N–C(16)	1.512(7)
Ti–M(1)[a]	2.036(6)	C(7)–C(12)	1.518(8)
Ti–C(1)	2.357(7)	C(13)–C(14)	1.529(9)
Ti–C(2)	2.381(6)	C(15)–C(16)	1.530(8)
Ti–C(3)	2.369(6)	O–C(14)	1.421(9)
Ti–C(4)	2.343(6)	O–C(15)	1.414(8)
Bond angles			
M(1)–Ti–C(6) [a]	105.3(2)	C(12)–N–Ti	108.2(3)
M(1)–Ti–N [a]	112.1(2)	C(13)–N–Ti	116.3(3)
M(1)–Ti–Cl(1) [a]	112.6(2)	C(16)–N–Ti	104.9(3)
M(1)–Ti–Cl(2) [a]	111.2(2)	C(7)–C(6)–Ti	117.1(4)
C(6)–Ti–N	74.4(2)	C(11)–C(6)–Ti	126.6(4)
C(6)–Ti–Cl(1)	86.9(2)	C(6)–C(7)–C(12)	116.1(5)
C(6)–Ti–Cl(2)	142.2(2)	C(8)–C(7)–C(12)	121.2(5)
N–Ti–Cl(1)	134.6(13)	C(7)–C(12)–N	108.5(4)
N–Ti–Cl(2)	83.0(12)	C(14)–C(13)–N	113.1(5)
Cl(1)–Ti–Cl(2)	88.0(6)	C(15)–C(16)–N	113.9(5)
C(12)–N–C(13)	110.1(4)	C(13)–C(14)–O	111.3(5)
C(12)–N–C(16)	109.2(4)	C(16)–C(15)–O	110.0(5)
C(13)–N–C(16)	107.9(5)	C(14)–O–C(15)	110.0(5)

[a] M(1) is the centroid of the C(1)-to-C(5) ring.

VI and **VII** show an averaged structure with equivalent ArCH_2N resonances and dialkylamino groups. At low temperatures the spectra indicate an asymmetric structure as expected for the solid state of **VI**.

In the ^{1}H- and ^{13}C{^{1}H}-NMR spectra of **VI** recorded in toluene-d_8 at −10 °C, the asymmetry of the molecule can be easily inferred (Table 6). The benzyl methylene protons give rise to two AB doublets and the *N*-methyl protons give rise to two singlets, for which the ^{13}C{^{1}H}-NMR spectrum also shows two signals. In the ^{13}C{^{1}H}-NMR spectrum of **VI** at −10 °C, the ArCH_2N carbon resonates at $\delta = 71.26$ ppm. The resonance of the TiCp carbons appears at $\delta = 120.60$ ppm. The C_6H_4 carbons give rise to signals at $\delta = 123.22$, 126.44, 126.50, 140.89 and 141.50 ppm. In addition, the spectrum shows a characteristic low-field chemical shift for the *C*1 carbon ($\delta = 199.71$ ppm). Similar values have been observed for a range of titanium(IV) arylaminate complexes [24,40,41]

At 60 °C, a time-averaged signal is observed for the methyl resonances ($\delta = 2.32$ ppm). In addition, the ArCH_2N protons give rise to a broad signal at $\delta =$ 2.90 ppm. From the coalescence temperature of the methyl resonances ($T_c = 42$ °C), the Gibbs free energy of activation was estimated ($\Delta G^{\ddagger} = 60.7(3)$ kJ mol^{-1}).

^{1}H- and ^{13}C{^{1}H}-NMR data for [TiCp($C_6H_4CH_2NEt_2$)Cl_2] (**VII**) are shown in Table 7. At −30 °C the ArCH_2N protons appear as two doublets, the NCH_2CH$_3$ protons give rise to two overlapping

Table 6
^{1}H- and ^{13}C{^{1}H}-NMR data for [TiCp($C_6H_4CH_2NMe_2$)Cl_2] (**VI**) in toluene-d_8 (in ppm, δ-scale, −10 °C)

Proton or carbon	Chemical shifts	
	^{1}H-NMR	^{13}C{^{1}H}-NMR
NCH_3	1.93 (s, 3H)	48.4
	2.47 (s, 3H)	51.2
ArCH_2N	2.39 (d, 1H, ^2J = 14.2 Hz)	71.3
	3.08 (d, 1H, ^2J = 14.2 Hz)	
TiCp	5.98 (s, 5H)	120.6
Position 3	6.55–6.57 (m, 1H)	123.2
Positions 4, 5	6.88–6.92 (m, 2H)	126.4
		126.5
Position 6	7.70–7.72 (m, 1H)	140.9
Position 2	–	141.5
Position 1	–	199.7

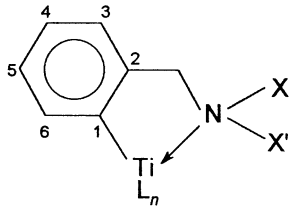

Representation of a titanium arylaminate complex, showing the numbering scheme.

multiplets and the methyl protons appear as two triplets, These broaden and then coalesce as the temperature rises, until finally a single sharp resonance is observed. The Gibbs free energy of activation at coalescence (T_c = −7 °C) for the methyl groups is 55.1(3) kJ mol^{-1}. The lower activation barrier for **VII** as compared to **VI** is probably due to the increase with the bulk of the amine substituents (Me → Et).

Table 7
^{1}H- and ^{13}C{^{1}H}-NMR data for [TiCp($C_6H_4CH_2NEt_2$)Cl_2] (**VII**) in toluene-d_8 (in ppm, δ-scale, −30 °C)

Proton or carbon	Chemical shifts	
	^{1}H-NMR	^{13}C{^{1}H}-NMR
NCH$_2CH_3$	0.42 (t, 3H, ^3J = 6.8 Hz)	10.4
	0.51 (t, 3H, ^3J = 6.8 Hz)	10.8
NCH_2CH$_3$	2.21 (m, 1H)	49.8
	3.21 (m, 2H)	56.6
	3.82 (m, 1H)	
ArCH_2N	2.89 (d, 1H, ^2J = 14.6 Hz)	60.5
	3.10 (d, 1H, ^2J = 14.6 Hz)	
TiCp	6.10 (s, 5H)	121.1
Position 3	6.63 (d, 1H, ^3J = 7.1 Hz)	123.0
Positions 4, 5	6.88–6.94 (m, 2H)	126.2
		126.3
Position 6	7.71 (d, 1H, ^3J = 7.2 Hz)	140.2
Position 2	–	140.7
Position 1	–	199.6

The ^{13}C{^{1}H}-NMR spectrum at −30 °C shows analogous splittings and temperature dependence. There is evidence from saturation transfer that the two ethyl groups exchange with each other. Upon irradiation at δ = 3.82 ppm there is magnetization transfer to δ = 2.21 ppm. In addition, a negative NOE (−7%) is observed at δ = 3.21 ppm. Furthermore, irradiation at δ = 6.10 ppm (attributed to the resonances of the Cp protons) produces a small effect on the signal at δ = 2.21 ppm (−2.7%), but it has no effect on the signal at δ = 3.82 ppm. This indicates that one of the ethyl groups is cis to the Cp ring, while the other is trans to the Cp. A negative NOE is also observed at δ = 2.89 and 3.10 ppm (−3.2 and −1.5%, respectively), which suggests that one of the ArCH_2N protons is close to the Cp ring, while the other is pointing away.

To explain the observed fluxional behaviour of **VI** and **VII** in solution (Scheme 2) two mechanisms are possible: dissociation of the Ti–N bond followed by rotation around the Ti–C1 bond, as suggested for [Ti(tbmp)($C_6H_4CH_2NMe_2$)Cl] ($\Delta G^{\ddagger}$ (15 °C) = 62.3 kJ mol^{-1}) [39], and a non-dissociative pseudorotation process as proposed for a series of pentacoordinate Si–N chelate complexes [35]. However, no clue is given by the present set of data as to the exact mechanism by which exchange is affected.

^{1}H-NMR data for the compound [TiCp{C_6H_4-$CH_2N(CH_2CH{=}CH_2)_2$}Cl_2] (**VIII**) are summarised in Table 8. At room temperature, the diastereotopic ArCH_2N protons and N($CH_2CH{=}CH_2$)$_2$ groupings are rendered equivalent through a fast exchange process.

^{1}H- and ^{13}C{^{1}H}-NMR data for the complex [TiCp($C_6H_4CH_2NC_4H_8O$)Cl_2] (**IX**) in toluene-d_8 at −50 °C are presented in Table 9. The assignment of the CH_2 resonances was supported by a COSY ^{1}H-NMR experiment. For the hydrogen-atom-labelling scheme used see Fig. 5. At −50 °C the compound is in the slow exchange regime and distinct signals are observed from each methylene proton. The ArCH_2N protons give rise to two signals. Because of the close proximity of the resonance at δ = 2.51 ppm to the resonance at δ = 2.48 ppm assigned to the A_{Ne} proton (^2J = 13.6 Hz), this signal appears as a triplet. The B_{Ne} proton is split into a doublet by coupling with the geminal B_{Na} proton. The B_{Na} proton appears as a multiplet by coupling with the geminal B_{Ne} and the

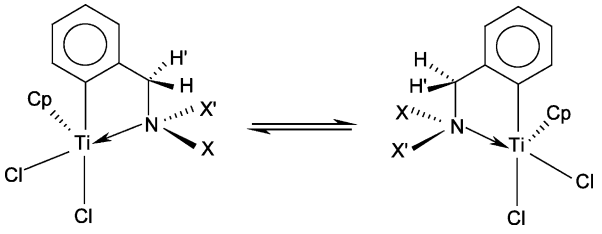

Scheme 2.

Table 8
^{1}H-NMR data for [TiCp{$C_6H_4CH_2N(CH_2CH{=}CH_2)_2$}$Cl_2$] (**VIII**) in C_6D_6 (in ppm, δ-scale, room temperature)

Proton	Chemical shifts
ArCH_2N	3.30 (s, 2H)
NCH_2CH=CH_2	3.98 (br, 4H)
NCH_2CH=CH_2	4.73 (d, 2H, J_{trans} = 16.2 Hz)
	4.83 (d, 2H, J_{cis} = 10.0 Hz)
NCH_2CH=CH_2	5.38–5.53 (m, 2H)
TiCp	6.20 (s, 5H)
Position 3	6.65 (m, 1H)
Positions 4, 5	6.95 (m, 2H)
Position 6	7.75 (m, 1H)

Table 9
^{1}H- and ^{13}C{^{1}H}-NMR data for [TiCp($C_6H_4CH_2NC_4H_8O$)Cl_2] (**IX**) in toluene-d_8 (in ppm, δ-scale, −50 °C)

Proton or carbon	Chemical shifts	
	^{1}H-NMR [a]	^{13}C{^{1}H}-NMR [b]
CH_2	1.27 (B_{Ne}, d, 1H, ^2J = 13.4 Hz)	48.7
	2.47–2.52 (A_{Ne}, $ArCH_2$, pt, 2H) [c]	53.6
	2.71 (A_{Oe}, m, 1H)	56.5
	2.97 (B_{Oe}, m, 1H)	59.5
	3.07 (A_{Oa}, B_{Oa}, m, 2H)	63.2
	3.57 ($ArCH_2$, d, 1H, ^2J = 14.7 Hz)	
	3.94 (B_{Na}, m, 1H)	
	4.62 (A_{Na}, m, 1H)	
TiCp	5.98 (s, 5H)	121.0
Position 3	6.59 (m, 1H)	123.8
Positions 4, 5	6.94 (m, 2H)	126.7
		128.3
Position 6	7.85 (m, 1H)	141.1
Position 2	–	141.0
Position 1	–	201.5

[a] For the hydrogen atom labelling scheme used see Fig. 4.16.
[b] The assignments of the ^{13}C resonances were supported by DEPT experiments.
[c] Two overlapping doublets; signal appears as a triplet.

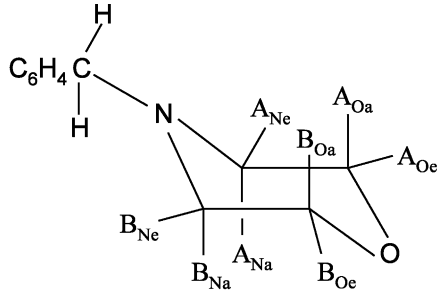

Fig. 5. Representation of a $C_6H_4CH_2NC_4H_8O$ moiety, showing the hydrogen atom labelling scheme; the subscripts a or e refer to the position of the hydrogen atom, axial or equatorial.

vicinal axial B_{Oa} and equatorial B_{Oe} (^3J = 4.1 Hz) protons. The B_{Oe} proton appears as a multiplet by coupling to the geminal B_{Oa} proton (^2J = 12.2 Hz) and the vicinal axial B_{Na} proton. The A_{Oe} proton gives rise to a multiplet (doublet of doublets) by coupling to the geminal A_{Oa} proton (^2J = 12.4 Hz) and the vicinal axial A_{Na} proton (^3J = 3.5 Hz). The multiplet at δ = 3.07 ppm is assigned to the axial OCH_2 protons. Finally, the A_{Na} proton is split into a multiplet. The ^{13}C{^{1}H} spectrum at −50 °C shows separate signals from all five methylene carbons.

At −50 °C there is evidence from saturation transfer that there is exchange between axial protons of the NC_4H_8O group. At higher temperature (−10 °C) there is exchange between axial and equatorial protons of the NC_4H_8O ring. This implies that the Cp ring is close to one side of the NC_4H_8O ring and not the other. Furthermore, one of the benzyl methylene protons is close to the Cp ring, while the other is pointing away.

For the observed fluxional behaviour of **IX** in solution two processes can be distinguished: a low-temperature process, which exchanges the geminal ArCH_2N protons; this process also exchanges the axial protons of the NC_4H_8O ring (A_{Na} with B_{Na} and A_{Oa} with B_{Oa}); and a higher-temperature process which exchanges the axial with the equatorial protons of the NC_4H_8O ring. The only plausible mechanism that can account for the latter process involves the dissociation of the Ti–N bond followed by inversion at the nitrogen atom, then rotation about the N–CH_2Ar bond, and finally recombination to form the Ti–N bond. This pathway was suggested to account for the fluxional behaviour observed for the titanium arylaminate complexes [Ti(η^5:η^1-$C_5Me_4SiMe_2NPr^i$)(C_6H_4-2-CH_2NMe_2)-Cl] and [Ti(η^5:η^1-$C_5Me_4SiMe_2NCH_2Ph$)(C_6H_4-2-CH_2-NMe_2)Cl] [24].

The rate of exchange is affected by the bulk of the substituents and solvents. In oxygen-containing solvents, such as thf, the exchange processes were faster. This suggests that thf probably assists the dissociation of the Ti–N bond (S_N2 type dissociation). At −50 °C all signals are sharp. At 70 °C the signals due to the C_6H_4 and TiCp protons are broad, while at 90 °C the absence of the TiCp signal (and the C_6H_4 resonances) may indicate the formation of paramagnetic species.

^{1}H-NMR data for [TiCp($C_6H_4CH_2NMeCH_2Ph$)Cl_2] (**X**) in thf-d_8 are displayed in Table 10. The assignments of the proton resonances were supported by COSY ^{1}H-NMR and NOE experiments. At −35 °C two isomers are present in solution, with the Cp ring either *cis* (isomer A) or *trans* (isomer B) to the $PhCH_2$ group (Fig. 6). At this temperature, the approximate ratio of the isomers A and B is 1.7:1 and the asymmetry of the molecule creates diastereotopic environments for the methylene protons. The C_6H_4 and C_6H_5 protons give rise to multiplets in the region δ = 6.88–7.87 ppm.

Table 10
^{1}H-NMR chemical shifts (selected data) for [TiCp($C_6H_4CH_2$N-MeCH$_2$Ph)Cl$_2$] (**X**) in thf-d_8 (in ppm, δ-scale, −35 °C)

Proton or carbon	Chemical shifts [a]	
	Major isomer (A)	Minor isomer (B)
CH_3	2.85 (s, 3H)	2.72 (s, 3H)
CH_2	3.33 (d, 1H, $^2J = 14.3$ Hz)	3.40 (s, 1H, $^2J = 15.0$ Hz)
	4.74 (d, 1H, $^2J = 14.3$ Hz)	4.08 (s, 1H, $^2J = 15.0$ Hz)
	4.33 (d, 1H, $^2J = 13.2$ Hz)	4.57 (s, 1H, $^2J = 13.2$ Hz)
	4.79 (d, 1H, $^2J = 13.2$ Hz)	5.14 (s, 1H, $^2J = 13.2$ Hz)
TiCp	6.86 (s, 5H)	6.76 (s, 5H)

[a] Assignments were supported by COSY ^{1}H-NMR and NOE experiments.

Another pair of isomers is present in a small proportion compared to the main pair of isomers. These may also be isomers of the major component, or a further compound. This gives rise to two singlets at $\delta = 2.75$ and 2.95 ppm due to the methyl resonances and to doublets at $\delta = 3.22$, 4.38, 4.46 (two overlapping doublets), 4.67 (two overlapping doublets), 4.86 and 5.03 ppm due to the methylene resonances. At high temperature all the pairs of signals of the four isomers coalesce, which indicates exchange between the minor and the major pair of isomers. However, we were not able to isolate the minor pair of isomers. Further studies are needed.

At −20 °C there is evidence from saturation transfer that the isomers A and B are exchanging with each other. This shows exchange between the methylene protons of isomers A and B. Increase of temperature brings about a second process which exchanges the geminal methylene protons of isomers A and B. As for the compound **IX**, the lower-temperature process can be assigned either to a non-dissociative pseudorotation reaction or to Ti–N bond dissociation followed by rotation about the Ti–C1 bond and complexation, while the higher temperature process is due to the reversible dissociation of the Ti–N bond followed by inversion at the nitrogen atom.

At 60 °C a single sharp signal is observed at $\delta = 2.82$ ppm assigned to the methyl protons. A single sharp signal is also observed for the TiCp protons at $\delta = 6.68$ ppm, while the methylene protons give rise to two broad signals at $\delta = 3.83$ and 4.72 ppm. From the coalescence temperature of the methyl resonances ($T_c = 24$ °C), the free energy of activation was estimated to be approximately 60.2 kJ mol^{-1}. This value is very close to that observed for **VII** ($\Delta G^{\ddagger}$ (42 °C) = 60.7 kJ mol^{-1}).

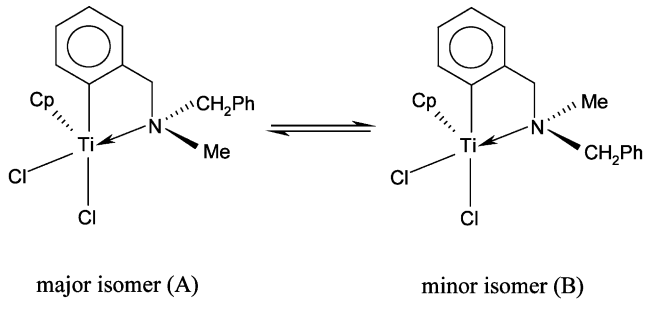

Fig. 6. Proposed isomers (major pair) for [TiCp($C_6H_4CH_2$N-MeCH$_2$Ph)Cl$_2$] (**X**).

3. Conclusions

Some titanium arylaminate complexes [TiCp(C_6H_4-CH$_2$R)Cl$_2$] (R = NMe$_2$ (**VI**), NEt$_2$ (**VII**), N(CH$_2$CH=CH$_2$)$_2$ (**VIII**), NC$_4$H$_8$O (**IX**) or NMeCH$_2$Ph (**X**)) have been synthesised in high yields. The compounds **VI**, **VIII** and **IX** possess distorted square-pyramidal coordination for the titanium. The Cp ring occupies an apical position, while the two chlorine atoms, the nitrogen atom and the ligating aryl carbon form the base of the pyramid. The substituents on the nitrogen do not seem to affect substantially the geometric parameters of **VI**, **VIII** and **IX**. Compounds The NMR spectra of **VI**–**X** exhibited dynamic behaviour. For **IX** and **X** two consecutive exchange processes were observed, one possibly involving a pseudorotation reaction, while the other process was assigned to Ti–N cleavage followed by inversion at the nitrogen atom. Furthermore, it was found that the exchange processes were much slower for **VI** than for **VII**–**X**. The relative exchange rates are **VI** < **X** < **VII** < **IX**.

[VCl$_2$(tmen)$_2$] reacts with two equivalents of the lithium arylaminates (except for LiC$_6$H$_4$CH$_2$N-(CH$_2$CH=CH$_2$)$_2$) with the uptake of N$_2$. No dinitrogen-containing products were isolated, but this is not entirely surprising, since this type of dinitrogen complex is not very stable and is difficult to characterise.

4. Experimental

All operations were carried out under an inert atmosphere in an argon-filled drybox or with use of standard Schlenk techniques. Solvents were dried by standard procedures [43] and distilled under N$_2$ prior to use, *n*-butyllithium (1.6 M solution in hexane) was obtained commercially and used fresh, [TiCpCl$_3$] [42] and [VCl$_2$(tmen)$_2$] [19] were prepared by literature methods. IR spectra were recorded on a Perkin–Elmer Spectrum One model FT-IR spectrometer, from Nujol mulls prepared under dinitrogen and spread on KBr plates. NMR spectra were obtained in the appropriate deuterated solvents using a Brüker 300 or 500 MHz instru-

ment. (^{13}C, ^{1}H)-HETCOR NMR, ^{1}H{^{1}H}-NOE and variable temperature Microanalyses were by Medac Ltd. or the University of Surrey. Mass spectra were taken by Dr. Ali Abdul-Sada, at the University of Sussex, using a Kratos M580RF instrument for FAB spectra (and 3-nitrobenzyl alcohol as a matrix material), and a Fisons VG Autospec for EI spectra.

X-ray crystal structure data were collected by the $2\theta-\omega$ scan method at 173(2) K using an Enraf–Nonius CAD4 diffractometer with. Mo–K_α ($\lambda = 0.71073$ Å) radiation. During processing, the data were corrected for absorption by semi-empirical ψ-scan methods. The structures were solved by direct methods in SHELXS and refined by full-matrix least-square methods in SHELXN [44] All non-hydrogen atoms were refined anisotropically. Diagrams of the molecular structure of complexes were drawn with the ORTEP package with ellipsoids drawn at 50% probability [45]. Details of the X-ray crystal structure determinations are shown in Table 11.

4.1. Synthesis of BrC_6H_4-2-CH_2NEt_2

This was carried out as a colourless liquid as described in Ref. [26] in 80% yield. ^{1}H-NMR ($CDCl_3$, ppm) δ: 0.98 (t, NCH_2CH_3, 6H, $^{3}J = 7.1$ Hz), 2.50 (q, NCH_2CH_3, 4H, $^{3}J = 7.1$ Hz), 3.56 (s, $C_6H_4CH_2N$, 2H), 6.98 (m, C_6H_4, 1H), 7.20 (m, C_6H_4, 1H), 7.42-7.48 (m, C_6H_4, 2H).

4.2. Synthesis of BrC_6H_4-2-$CH_2N(CH_2CH{=}CH_2)_2$

As for the synthesis of BrC_6H_4-2-CH_2NEt_2 with $HN(CH_2CH{=}CH_2)_2$ (9.8 cm^3, 79.4 mmol) and 2-bromobenzyl bromide (6.32 g, 25.3 mmol), affording after distillation a colourless oil (5.18 g, 19.5 mmol, 77% yield). ^{1}H-NMR ($CDCl_3$, ppm) δ: 3.05 (d, $NCH_2CH{=}CH_2$, 4H, $^{3}J = 6.1$ Hz), 3.56 (s, $C_6H_4CH_2N$, 2H), 5.02–5.18 (m, $NCH_2CH{=}CH_2$, 4H), 5.72–5.88 (m, $NCH_2CH{=}CH_2$, 2H), 6.98 (m, C_6H_4, 1H), 7.19 (m, C_6H_4, 1H), 7.39–7.50 (m, C_6H_4, 2H). ^{13}C{^{1}H}-NMR ($CDCl_3$, ppm) δ: 56.66 ($NCH_2CH{=}CH_2$), 56.88 ($C_6H_4CH_2N$), 117.48 ($NCH_2CH{=}CH_2$), 124.16 (C1), 127.18 (C5), 128.09 (C4), 130.38 (C3), 132.50 (C6), 135.54 ($NCH_2CH{=}CH_2$), 138.74 (C2). The assignment of the C1–C6 resonances was based on Ref. [26] (see Table 6).

4.3. Synthesis of BrC_6H_4-2-$CH_2NC_4H_8O$

As for the synthesis of BrC_6H_4-2-CH_2NEt_2 with HNC_4H_8O (5.9 cm^3, 67.7 mmol) and o-bromobenzyl bromide (5.47 g, 21.9 mmol), affording after distillation under vacuum a colourless oil (4.31 g, 16.8 mmol, 77% yield). ^{1}H-NMR ($CDCl_3$, ppm) δ: 2.47 (t, NCH_2, 4H, $^{3}J = 4.7$ Hz), 3.54 (s, $C_6H_4CH_2N$, 2H), 3.67 (t, OCH_2, 4H, $^{3}J = 4.7$ Hz), 7.06 (m, C_6H_4, 1H), 7.22 (m, C_6H_4, 1H), 7.40–7.50 (m, C_6H_4, 2H). ^{13}C{^{1}H}-NMR ($CDCl_3$, ppm) δ: 53.50 (NCH_2), 62.10 ($C_6H_4CH_2N$), 67.00 (OCH_2), 124.65 (C1), 127.12 (C5), 128.42 (C4), 130.67 (C3), 132.70 (C6), 137.1 (C2). The assignment of the C1–C6 resonances was based on Ref. [26] (see Table 6).

4.4. Synthesis of BrC_6H_4-2-CH_2NMeCH_2Ph

As for the synthesis of BrC_6H_4-2-CH_2NEt_2, from $HMeCH_2Ph$ (11 cm^3, 85.2 mmol) and 2-bromobenzyl bromide (6.85 g, 27.4 mmol). A pale yellow oil was obtained after distillation under vacuum (5.95 g, 20.5 mmol, 75% yield). ^{1}H-NMR ($CDCl_3$, ppm) δ: 2.28 (s, NCH_3, 3H), 3.67 (s, NCH_2, 2H), 3.71 (s, NCH_2, 2H), 7.12–7.64 (m, Ar–H, 9H). ^{13}C{^{1}H}-NMR ($CDCl_3$, ppm) δ: 42.09 (NCH_3), 61.04 (NCH_2), 62.10 (NCH_2), Ar–C: 124.52 (C–Br), 126.93, 127.18, 128.18 (C_6H_5), 128.26, 128.83 (C_6H_5), 130.70, 132.64, 138.46 (C_{ipso}), 139.19 (C_{ipso}).

4.5. Synthesis of LiC_6H_4-2-CH_2NMe_2 (*I*)

This was prepared as white powder in 73% yield following the procedure of Ref. [25].

4.6. Synthesis of LiC_6H_4-2-CH_2NEt_2 (*II*)

This was prepared as a white powder in 74% yield following the procedure of Ref. [26]. ^{1}H-NMR (C_6D_6, ppm) δ: 0.17 (t, NCH_2CH_3, 3H, $^{3}J = 7.1$ Hz), 0.63 (t, NCH_2CH_3, 3H, $^{3}J = 7.1$ Hz), 1.94 (m, NCH_2CH_3, 2H), 2.29 (m, NCH_2CH_3, 2H), 3.27 (d, $C_6H_4CH_2N$, 1H, $^{2}J = 13.0$ Hz), 4.57 (d, $C_6H_4CH_2N$, 1H, $^{2}J = 13.0$ Hz), 7.15–7.31 (m, C_6H_4, 3H), 8.49 (d, H6, 1H, $^{3}J = 5.5$ Hz). ^{13}C{^{1}H}-NMR (C_6D_6, ppm) δ: 7.13 (NCH_2CH_3), 9.92 (NCH_2CH_3), 43.89 (NCH_2CH_3), 46.58 (NCH_2CH_3), 63.71 ($C_6H_4CH_2N$), 125.31 (C3), 126.80 (C5), 127.70 (C4), 140.14 (C6), 152.48 (C2); C1 not observed. The assignment of the C1–C6 resonances was based on Ref. [26] (see Table 6).

4.7. Synthesis of LiC_6H_4-2-$CH_2N(CH_2CH{=}CH_2)_2$ (*III*)

To a solution of BrC_6H_4-2-$CH_2N(CH_2CH{=}CH_2)_2$ (5.18 g, 19.5 mmol) in hexane (20 cm^3), a solution of *n*-butyllithium in hexane (1.6 M, 12 cm^3, 19.4 mmol) was added slowly at room temperature (r.t.). After stirring the reaction mixture for ca. 24 h, the solvent was concentrated under vacuum to ca. 15 cm^3, and the resulting white precipitate was filtered off and dried under vacuum (2.21 g, 11.4 mmol, 59% yield). The product is quite soluble in hexane. Cubic crystals suitable for X-ray structural determination

Table 11
Details of crystal structure determinations

	[{$LiC_6H_4CH_2N(CH_2$-$CH{=}CH_2)_2$}$_4$] (**III**)	[$TiCp(C_6H_4CH_2NMe_2)Cl_2$] (**VI**)	[$TiCp\{C_6H_4CH_2N(CH_2$-$CH{=}CH_2)_2\}Cl_2$] (**VIII**)	[$TiCp(C_6H_4CH_2NC_4H_8O)Cl_2$] (**IX**)
Formula	$C_{52}H_{64}Li_4N_4$	$C_{14}H_{17}Cl_2NTi$	$C_{18}H_{21}Cl_2NTi$	$C_{16}H_{19}Cl_2NOTi$
M (g mol^{-1})	772.83	318.1	370.16	360.12
Crystal system	Tetragonal	Orthorhombic	Orthorhombic	Orthorhombic
Crystal size (mm^3)	$0.30 \times 0.30 \times 0.30$	$0.40 \times 0.20 \times 0.20$	$0.30 \times 0.10 \times 0.05$	$0.30 \times 0.30 \times 0.05$
Space group	$I4_1/a$ (no. 88)	*Pbca* (no. 61)	$P2_12_12_1$ (no. 19)	*Pbca* (no. 61)
Unit cell dimensions				
a (Å)	19.8192(8)	13.525(3)	10.0949(8)	13.5701(8)
b (Å)	19.8192(8)	14.366(4)	13.1163(10)	15.9994(12)
c (Å)	11.9344(6)	14.775(6)	13.2553(6)	14.8655(13)
α (°)	90	90	90	90
β (°)	90	90	90	90
γ (°)	90	90	90	90
V (Å^3)	4687.8(4)	2871(2)	1755.1(2)	3227.5(4)
Z	4	8	4	8
D_{calc} (g cm^{-3})	1.10	1.47	1.40	1.48
μ (mm^{-1})	0.06	0.95	0.79	0.86
$F(000)$	1664	1312	768	1488
Range for data collection θ (°)	$3.71 \leq \theta \leq 22.98$	$2 \leq \theta \leq 25$	$3.70 \leq \theta \leq 25.00$	$3.74 \leq \theta \leq 22.99$
Index ranges	$-21 \leq h \leq 21$, $-21 \leq k \leq 21$, $-13 \leq l \leq 11$	$0 \leq h \leq 16$, $0 \leq k \leq 17$, $0 \leq l \leq 17$	$-10 \leq h \leq 12$, $-12 \leq k \leq 15$, $-15 \leq l \leq 15$	$-14 \leq h \leq 14$, $-17 \leq k \leq 16$, $-13 \leq l \leq 16$
Unique reflections	1617	2541	3080	2216
Observed ($I > 2\sigma(I)$)	1209	1912	2643	1768
Final R_1, wR_2 ($I > 2\sigma(I)$)	0.077; 0.200	0.071; 0.183	0.046; 0.103	0.062; 0.121
R_1, wR_2 (all data)	0.101; 0.223	0.093; 0.205	0.057; 0.109	0.082; 0.128

were obtained by cooling the filtrate at −20 °C for 7 days.

4.8. Synthesis of LiC_6H_4-2-$CH_2NC_4H_8O$ (*IV*)

This was prepared as a white powder in 90% yield following the procedure used for (**II**). LiC_6H_4-2-$CH_2NC_4H_8O$ is insoluble in hexane, Et_2O and benzene and it is readily soluble in thf. ^{1}H-NMR (thf-d_8, ppm) δ: 2.36 (m, NCH_2, 2H), 2.49 (s, br, NCH_2, 2H), 3.45–3.60 (m, OCH_2 and $C_6H_4CH_2N$, 6H), 6.77–6.84 (m, C_6H_4, 2H), 7.20–7.32 (m, C_6H_4, 1H), 7.91 (m, H6, 1H).

4.9. Synthesis of LiC_6H_4-2-CH_2NMeCH_2Ph (*V*)

As for the synthesis of (**II**) as a cream-coloured powder, in 90% yield. This product is insoluble in hexane, Et_2O or benzene, and it is soluble in thf. ^{1}H-NMR (thf-d_8, ppm, 50 °C) δ: 1.87 (s, NCH_3, 3H), 3.61 (s, $NCH_2C_6H_5$, 2H), 3.82 (s, $C_6H_4CH_2N$, 2H), 6.94–7.42 (m, C_6H_4 and C_6H_5, 8H), 8.10 (d, C_6H_4–H6, 1H, $^3J = 5.2$ Hz). The ^{1}H-NMR spectrum at r.t. was also recorded, the same peaks are observed but they are much broader. $^{13}C\{^1H\}$-NMR (thf-d_8, ppm, 25 °C) δ: 40.54 (NCH_3), 64.52 ($NCH_2C_6H_5$), 71.97 ($C_6H_4CH_2N$), Ar–C: 123.98, 124.29, 126.05, 127.57, 128.56 (C_6H_5), 131.56 (C_6H_5), 137.96 (C_6H_5–C_{ipso}), 144.30, 151.60 (C_6H_4–C_{ipso}), 189.20 (C–Li).

4.10. Synthesis of [$TiCp(C_6H_4CH_2NMe_2)Cl_2$] (*VI*)

To a yellow solution of [$TiCpCl_3$] (0.95 g, 4.30 mmol) in Et_2O (70 cm^3), solid LiC_6H_4-2-CH_2NMe_2 (0.68 g, 4.82 mmol) was added. An orange precipitate formed immediately after the addition. The mixture was allowed to react for 3 h at r.t. and then it was filtered. The orange powder was extracted with hot toluene and filtered (20 cm^3). The light-brown residue on the sinter (LiCl) was discarded. Red crystals suitable for X-ray diffraction study separated upon cooling the filtrate slowly to r.t. Yield: 0.90 g, 66% (Found: C, 52.4; H, 5.45; N, 4.50. $C_{14}H_{17}Cl_2NTi$ requires: C, 52.86; H, 5.39; N, 4.40%). IR (cm^{-1}): 760 (s), 831 (s), 857 (m), 982 (m), 1024 (m), 1099 (w), 1263 (w), 1402 (w), 3115 (w). EIMS: 316 (18%) $[M-H]^+$; 282 (90) $[M-Cl]^+$; 183 (51) $[TiCpCl_2]^+$; 134 (100) $[C_6H_4CH_2R]^+$; 58 (86) $[CH_2R]^+$; 91 (92) $[C_6H_5CH_2]^+$; 65 (88) Cp^+.

4.11. Synthesis of [TiCp($C_6H_4CH_2NEt_2$)Cl_2] (**VII**)

To a yellow solution of [$TiCpCl_3$] (0.80 g, 3.64 mmol) in Et_2O (50 cm^3), one portion of LiC_6H_4-2-CH_2NEt_2 (0.61 g, 3.61 mmol) was added as a solid. An orange precipitate formed immediately. The reaction mixture was continued to stir for 4 h and then it was filtered. The orange powder isolated was extracted with toluene (15 cm^3). Red crystals of **VII** separated by layering the toluene extract with hexane (30 cm^3). A second crop of red crystalline solid was isolated from the mother liquor after allowing it to stand at −20 °C for 3 days. Yield: 0.9 g, 2.61 mmol, 72% (Found: C, 55.1; H, 6.05; N, 4.20. $C_{16}H_{21}Cl_2NTi$ requires: C, 55.52; H, 6.11; N, 4.05%). Complex **VII** is insoluble in hexane, slightly soluble in Et_2O and readily soluble in toluene. It gradually decomposes in thf at r.t. (2–4 days). At low temperature (−20 °C), decomposition also occurs but is slower (1–2 weeks). IR (cm^{-1}): 741 (s), 829 (s), 869 (m), 1018 (m), 1046 (m), 1083 (m), 1103 (m), 1261 (m), 3077 (w). EIMS: 344 (48%) $[M-H]^+$; 310 (80) $[M-HCl]^+$; 164 (61) $[(C_6H_5CH_2R)H]^+$; 149 (83) $[TiCpCl]^+$; 72 (30) $[CH_2R]^+$; 92 (77) $[C_6H_5CH_2]^+$; 65 (80) Cp^+; 29 (100) Et^+.

4.12. Synthesis of [TiCp{$C_6H_4CH_2N(CH_2CH{=}CH_2)_2$}$Cl_2$] (**VIII**)

To a yellow solution of [$TiCpCl_3$] (0.80 g, 3.64 mmol) in Et_2O (50 cm^3), one portion of the solid LiC_6H_4-2-$CH_2N(CH_2CH{=}CH_2)_2$ (0.70 g, 3.63 mmol) was added. The colour of the reaction mixture changed immediately from yellow to red. The reaction was carried out for 2 h and the mixture was then filtered. In this manner, 0.25 g of a purple powder (A) were isolated. The volume of the filtrate was reduced under vacuum to ca. 20 cm^3. The brick-red powder that precipitated out was filtered, quickly washed with hexane (2×10 cm^3) and dried under vacuum for 2 h. Yield: 0.70 g, 1.89 mmol, 52% (Found: C, 57.6; H, 5.75; N, 3.90. $C_{18}H_{21}Cl_2NTi$ requires: C, 58.41; H, 5.72; N, 3.78%). Recrystallisation from a concentrated thf/Et_2O/hexane solution (1:1:1) afforded red crystals of **VIII** suitable for X-ray diffraction analysis. These crystals were isolated as soon as they formed (ca. 2 h). After longer periods (10–15 h) the solution changes from brick-red to greenish-brown, with formation of pale green and deep blue crystals. Preliminary X-ray structural analyses showed these crystals to be [$TiCl_3(thf)_3$] and [$TiCpCl_2(thf)_x$], respectively.

The solid (A) is apparently a mixture of LiCl and [$TiCpCl_2$]. Recrystallisation from a concentrated thf solution at 0 °C afforded the known complex [$TiCpCl_2(thf)_{1.5}$] as sky-blue crystals (0.21 g, 0.72 mmol, 20%). IR (**VIII**, cm^{-1}): 749 (s), 807 (s), 820 (s), 862 (m), 932 (m), 1020 (s), 1096 (m), 1261 (m). EIMS: 183 (90%) $[TiCpCl_2]^+$; 148 (100) $[TiCpCl]^+$; 91 (51) $[C_6H_5CH_2]^+$; 65 (93) 29 (100)

4.13. Synthesis of [TiCp($C_6H_4CH_2NC_4H_8O$)Cl_2] (**IX**)

As for the synthesis of [$TiCp(C_6H_4CH_2NMe_2)Cl_2$] (**VI**) with [$TiCpCl_3$] (0.80 g, 3.64 mmol), LiC_6H_4-2-$CH_2NC_4H_8O$ (0.67 g, 3.66 mmol) and Et_2O (100 cm^3). The orange powder isolated was washed with Et_2O (20 cm^3) and dried under vacuum for 2 h (0.95 g, 2.64 mmol, 72% yield). Recrystallisation from a thf solution layered with Et_2O (1:2) afforded red crystals suitable for X-ray structural analysis. Complex **IX** is only slightly soluble in toluene and is readily soluble in thf. It gradually decomposes in thf (solution changes from orange to greenish-brown over the period of 3–5 days). IR (cm^{-1}): 754 (s), 786 (s), 800 (s), 828 (s), 851 (m), 959 (m), 1020 (s), 1051 (s), 1098 (shoulder), 1113 (s), 1261 (s), 1289 (m). EIMS: 359 (4%) M^+; 324 (16) $[M-Cl]^+$; 183 (17) $[TiCpCl_2]^+$; 176 (67) $[C_6H_4CH_2R]^+$; 148 (34) $[TiCpCl]^+$; 100 (37) $[CH_2R]^+$; 91 (100) $[C_6H_5CH_2]^+$; 65 (54) Cp^+. Accurate mass measurement (EI): 358.028. Calculated for $C_{16}H_{18}Cl_2NOTi$ (M−H): 358.025.

4.14. Synthesis of [TiCp($C_6H_4CH_2NMeCH_2Ph$)Cl_2] (**X**)

As for the synthesis of [$TiCp(C_6H_4CH_2NMe_2)Cl_2$] (**VI**) with [$TiCpCl_3$] (0.80 g, 3.64 mmol), LiC_6H_4-2-CH_2NMeCH_2Ph (0.79 g, 3.64 mmol) and Et_2O (100 cm^3). The orange powder isolated was washed with Et_2O (20 cm^3) and dried under vacuum for 2 h (1.02 g, 2.59 mmol, 71% yield). Recrystallisation from a thf solution layered with hexane (1:2) afforded complex **X** as thin orange needles. Compound **X** is insoluble in Et_2O, hexane or toluene. It gradually decomposes in thf (solution changes from orange to greenish brown). Pale green crystals separate from a thf/Et_2O solution after allowing it to stand at r.t. for 3–4 days. IR (cm^{-1}): 703 (m), 738 (m), 752 (s), 832 (s), 861 (m), 1024 (s), 1054 (m), 1072 (m), 1095 (m), 1261 (m), 3112 (m). EIMS: 393 (3%) M^+; 357 (44) $[M-HCl]^+$; 183 (15) $[TiCpCl_2]^+$; 210 (60) $[C_6H_4CH_2R]^+$; 148 (35) $[TiCpCl]^+$; 134 (31) $[CH_2R]^+$; 91 (100) $[C_6H_5CH_2]^+$; 65 (63) Cp^+. Accurate mass measurement (EI): 392.04. Calculated for $C_{20}H_{20}Cl_2NTi$ (M−H): 392.05.

Acknowledgements

We acknowledge the award of an EPSRC Studentship to M. T.

References

[1] P.B. Hitchcock, G.J. Leigh, M. Togrou, J. Organomet. Chem. 664 (2002) 245.
[2] P.N. Jones, M.F. Zinn, C.R. Hauser, J. Org. Chem. 28 (1963) 663.
[3] J.T.B.H. Jastrzebski, F. van Koten, M. Konijn, C.H. Stam, J. Am. Chem. Soc. 104 (1982) 5490.
[4] E. Wehman, J.T.B.H. Jastrzebski, J.-M. Ernsting, D.M. Grove, G. van Koten, J. Organomet. Chem. 353 (1988) 145.
[5] E. Wehman, J.T.B.H. Jastrzebski, J.-M. Ernsting, D.M. Grove, G. van Koten, J. Organomet. Chem. 353 (1988) 133.
[6] L.E. Manzer, R.C. Gearheart, L.J. Guggenberger, J.F. Whitney, J. Chem. Soc. Chem. Commun. (1976) 942.
[7] (a) F.A. Cotton, G.N. Mott, Organometallics 1 (1982) 38;
(b) K. Angermund, K.H. Claus, R. Goddard, C. Krüger, Angew. Chem. Int. Ed. Engl. 24 (1985) 237;
(c) J.J.H. Edema, S. Gambarotta, A. Meetsma, A.L. Spek, Organometallics 11 (1992) 2452.
[8] F.A. Cotton, G.N. Mott, Inorg. Chem. 20 (1981) 3896.
[9] (a) P.A. van der Schaaf, W.J.J. Smeets, A.L. Spek, G. van Koten, J. Chem. Soc. Chem. Commun. (1992) 717;
(b) P.A. van der Schaaf, J. Boersma, H. Kooijman, A.L. Spek, G. van Koten, Organometallics 12 (1993) 4334;
(c) P.A. van der Schaaf, D.M. Grove, W.J.J. Smeets, A.L. Spek, G. van Koten, Organometallics 12 (1993) 3995.
[10] (a) R.G. Little, R.J. Doedens, Inorg. Chem. 12 (1973) 844;
(b) J.L. Latten, R.S. Dickson, G.B. Deacon, B.O. West, E.R.T. Tiekink, J. Organomet. Chem. 435 (1992) 101.
[11] A.A.H. van der Zeijden, G. van Koten, J.M.A. Wouters, W.F.A. Wijsmuller, D.M. Grove, W.J.J. Smeets, A.L. Spek, J. Am. Chem. Soc. 110 (1988) 5354.
[12] (a) C. Arlen, M. Pfeffer, O. Bars, D. Grandjean, J. Chem. Soc. Dalton Trans. (1983) 1535;
(b) P. Braunstein, D. Matt, D. Nobel, S.-E. Bouaoud, D. Grandjean, J. Organomet. Chem. 301 (1986) 401;
(c) S.-E. Bouaoud, P. Braunstein, D. Grandjean, D. Matt, D. Nobel, J. Chem. Soc. Chem. Commun. (1987) 488;
(d) T. Janecki, J.A.D. Jeffreys, P.L. Pauson, A. Pietrzykowski, Organometallics 6 (1987) 1553;
(e) J. Andrieu, P. Braunstein, Y. Dusausoy, N.E. Ghermani, Inorg. Chem. 35 (1996) 7174;
(f) P. Bhattacharyya, A.M.Z. Slawin, M.B. Smith, J. Chem. Soc. Dalton Trans. (1998) 2467;
(g) J. Ruiz, N. Gutillas, V. Rodríquez, J. Sampedro, G. López, P.A. Chaloner, P.B. Hitchcock, J. Chem. Soc. Dalton Trans. (1999) 2939;
(h) L.R. Falvello, M.M. Garcia, I. Lazaro, R. Navarro, E.P. Urriolabeitia, New J. Chem. 23 (1999) 227;
(i) J.-F. Ma, Y. Yamamoto, Inorg. Chim. Acta 299 (2000) 164.
[13] (a) A.F.M.J. van der Ploeg, G. van Koten, K. Vrieze, A.L. Spek, Inorg. Chem. 21 (1982) 2014;
(b) A.D. Ryabov, L.G. Kuz'mina, N.V. Dvortsova, D.J. Stufkens, R. van Eldik, Inorg. Chem. 32 (1993) 3166.
[14] (a) G. van Koten, J.T.B.H. Jastrzebski, F. Muller, C.H. Stam, J. Am. Chem. Soc. 107 (1985) 697;
(b) M.D. Janssen, M.A. Corsten, A.L. Spek, D.M. Grove, G. van Koten, Organometallics 15 (1996) 2810;
(c) C.M.P. Kronenburg, J.T.B.H. Jastrzebski, A.L. Spek, G. van Koten, J. Am. Chem. Soc. 120 (1998) 9688.
[15] (a) J. Vicente, M.T. Chicote, M.D. Bermúdez, P.G. Jones, G.M. Sheldrick, J. Chem. Res. 72 (1985) 954;
(b) J. Vicente, M.T. Chicote, M.D. Bermúdez, P.G. Jones, C. Fittschen, G.M. Sheldrick, J. Chem. Soc. Dalton Trans. (1986) 2361;
(c) J. Mack, K. Ortner, U. Abram, R.V. Parish, Z. Anorg. Allg. Chem. 623 (1997) 873;
(d) M.B. Dinger, W. Henderson, J. Organomet. Chem. 560 (1998) 233;
(e) U. Abram, K. Ortner, R. Gust, K. Sommer, J. Chem. Soc. Dalton Trans. (2000) 735.
[16] C. Arlen, M. Pfeffer, O. Bars, G. Le Borgne, J. Chem. Soc. Dalton Trans. (1986) 359.
[17] J.J.H. Edema, A. Meetsma, S. Gambarotta, J. Am. Chem. Soc. 111 (1989) 6878.
[18] A.L. Spek, J.J.H. Edema, S. Gambarotta, Acta Crystallogr. Sect. C 50 (1994) 1209.
[19] J.J.H. Edema, W. Stauthamer, F. van Bolhuis, S. Gambarotta, W.J.J. Smeets, A.L. Spek, Inorg. Chem. 29 (1990) 1302.
[20] C.P. Gerlach, J. Arnold, J. Chem., Soc. Dalton Trans. (1997) 4795.
[21] D. Ytsma, J.G. Hartsuiker, J.H. Teuben, J. Organomet. Chem. 74 (1974) 239.
[22] W.F.J. van der Wal, H.R. van der Wal, J. Organomet. Chem. 153 (1978) 335.
[23] M.S. Goedheijt, T. Nijbacker, O.S. Akkerman, F. Bickelhaupt, N. Veldman, A.L. Spek, J. Organomet. Chem. 527 (1997) 1.
[24] T. Eberle, T.P. Spaniol, J. Okuda, Eur. J. Inorg. Chem. (1998) 237.
[25] L.E. Manzer, J. Am. Chem. Soc. 100 (1978) 8068.
[26] I.C.M. Wehman-Ooyevaar, I.F. Luitwieler, K. Vatter, D.M. Grove, W.J.J. Smeets, E. Horn, A.L. Spek, G. van Koten, Inorg. Chim. Acta 252 (1996) 55.
[27] H. Köster, D. Thoennes, E. Weiss, J. Organomet. Chem. 160 (1978) 1.
[28] H. Hope, P.P. Power, J. Am. Chem. Soc. 105 (1983) 5320.
[29] B. Schubert, E. Weiss, Angew. Chem. Int. Ed. Engl. 95 (1983) 499.
[30] A.L. Spek, A.J.M. Duisenberg, G.W. Klumpp, P.J.A. Geurink, Acta Crystallogr. Sect. C 40 (1984) 372.
[31] K.S. Lee, P.G. Williard, J.W. Suggs, J. Organomet. Chem. 299 (1986) 311.
[32] D. Thoennes, E. Weiss, Chem. Ber. 111 (1978) 3157.
[33] D. Thoennes, E. Weiss, Chem. Ber. 111 (1978) 3726.
[34] G. van Koten, J.G. Noltes, J. Organomet. Chem. 174 (1979) 367.
[35] (a) G. van Koten, J.G. Noltes, J. Am. Chem. Soc. 101 (1979) 6593;
(b) S. Toyota, M. Oki, Bull. Chem. Soc. Jpn. 64 (1991) 1554;
(c) I. Kalikhman, S. Krivonos, A. Ellern, D. Kost, Organometallics 15 (1996) 5073.
[36] (a) P.B. Hitchcock, D.L. Hughes, G.J. Leigh, J.R. Sanders, J.S. de Souza, J. Chem. Soc. Dalton Trans. (1999) 1161;
(b) G.J. Leigh, R. Prieto-Alcón, J.R. Sanders, J. Chem. Soc. Chem. Commun. (1991) 921.
[37] R.S.P. Coutts, R.L. Martin, P.C. Wailes, Aust. J. Chem. 24 (1971) 2533.
[38] (a) J.H. Teuben, H.J. de Liefde Meijer, J. Organomet. Chem. 46 (1972) 313;
(b) J.H. Teuben, J. Organomet. Chem. 69 (1974) 241;
(c) E. Klei, J.H. Telgen, J.H. Teuben, J. Organomet. Chem. 209 (1981) 297.
[39] S. Fokken, T.P. Spaniol, H.-C. Kang, W. Massa, J. Okuda, Organometallics 15 (1996) 5069.
[40] E.E.C.G. Gielens, T.W. Dijkstra, P. Berno, A. Meetsma, B. Hessen, J.H. Teuben, J. Organomet. Chem. 591 (1988) 88.
[41] D. Cozak, M. Melnik, Coord. Chem. Rev. 74 (1986) 53.
[42] R.D. Gorsich, J. Am. Chem. Soc. 80 (1958) 4744.
[43] P.D. Perrin, W.L.F. Armarego, Purification of Laboratory Chemicals, 3rd ed., Pergamon Press, New York, 1988.

[44] (a) G.M. Sheldrick, SHELX-76, Program for Crystal Structure Determination, University of Cambridge, 1976;
(b) G.M. Sheldrick, SHELXN, an extended version of SHELX, University of Cambridge, 1977;
(c) G.M. Sheldrick, SHELXS, Program for Crystal Structure Determination, University of Göttingen, Germany, 1986;
(d) G.M. Sheldrick, Acta Crystallogr. Sect. A 46 (1990) 467;
(e) G.M. Sheldrick, SHELX-93, Program for crystal structure Refinement, University of Göttingen, 1993.
[45] C.K. Johnson, ORTEP, Program for Diagrams, Report ORNL-3794, Oak Ridge Laboratory, TN, revised in 1971.